Energy Optimization in Wireless Medical Systems Using Physiological Behavior

Hyduke Noshadi, Foad Dabiri, Saro Meguerdichian,
Miodrag Potkonjak and Majid Sarrafzadeh
Computer Science Department
University of California, Los Angeles, California, United States
{hyduke, dabiri, saro, miodrag, majid}@cs.ucla.edu

ABSTRACT

Wearable sensing systems are becoming widely used for a variety of applications, including sports, entertainment, and military. These systems have recently enabled a variety of medical monitoring and diagnostic applications in Wireless Health. The need for multiple sensors and constant monitoring lead these systems to be power hungry and expensive, with short operating lifetimes. In this paper, we introduce a novel methodology that takes advantage of the influence of human behavior on signal properties and reduces those three metrics from the data size point of view. This, in turn, directly influences the wireless communication and local processing power consumption. We exploit intrinsic space and temporal correlations between sensor data while considering both user and system behavior. Our goal is to select a small subset of sensors to accurately capture and/or predict all possible signals of a fully instrumented wearable sensing system. Our approach leverages novel modeling, partitioning, and behavioral optimization, which consists of signal characterization, segmentation and time shifting, mutual signal prediction, and subset sensor selection. We demonstrate the effectiveness of the technique on an insole instrumented with 99 pressure sensors placed in each shoe, which cover the bottom of the entire foot, resulting in energy reduction of 56% to 96% for error rates of 5% to 17.5%.

Categories and Subject Descriptors

C.3 [**Special-Purpose and Application-Based Systems**]: [Real-time and embedded systems]; B.8.2 [**Performance and Reliability**]: Performance Analysis and Design Aids; J.3 [**Life and Medical Sciences**]: Medical information systems

General Terms

Design, Algorithm, Performance

Keywords

Wearable Medical Systems, Energy Optimization, Sensor Selection, Behavioral Sensing.

Wireless Health '10, October 5–7, 2010, San Diego, USA

1. INTRODUCTION

Embedded networked systems and wide area cellular wireless systems are becoming ubiquitous in applications ranging from environmental monitoring to urban sensing. Meanwhile, sensor networks have emerged as an important class of distributed embedded systems capable of solving a variety of challenging monitoring and control problems in a number of application domains, ranging from government and military applications to seismic, habitat, and wildlife continuous observations. These technologies have recently been adopted to support the emerging work in medical devices equipped with sensors, known collectively as Wireless Health [1] [2] [3] [4]. Wireless Health merges data, knowledge, and wireless communication technologies to provide health care and medical services such as prevention, diagnosis, and rehabilitation outside of the traditional medical enterprise.

Such sensor systems have high potential to significantly improve the quality of life for large segments of the population and enable conceptually new types of applications. However, it is important to note that a path to industrial realization has been more elusive than initially was expected due to a variety of issues, including system and operational complexity, cost and energy sensitivity, semantic complexity, and the need for often revolutionary changes in consumer behavior. Ever-increasing opportunities in health care have thus motivated researchers in Computer Science and Electrical Engineering to develop technologies that can be adopted in the medical and physiological fields and to serve the recently growing demand of low cost and widely accessible health care services.

In this paper, we show how signal processing techniques (time-shifting and segmentation), in addition to a new combinatorial optimization paradigm (pseudo-exhaustive combinatorial search), can be used to design an energy optimized embedded sensing system to reduce energy consumption by more than an order of magnitude. While some of these techniques best perform on embedded sensing systems that share local communication, a majority of them can be applied on essentially any sensing systems. Our goal is to demonstrate that often expensive wearable sensing systems used in medical studies can be made more attractive to daily usage through a system of coordinated design and operational techniques that facilitate mass production, customization to specific customers, and low power operation.

Specifically, our optimization goal is to simultaneously minimize the cost (i.e. the number of sensors) and energy consumption (i.e. the weighted sum of collected and communi-

cated samples) while preserving a specified accuracy of collected data, or vice versa. To do so, we exploit intrinsic space and temporal correlations between sensor data while considering both user and system behavior. Our proposed methodology takes advantage of signal semantics and predictability among sensors to reduce the number of sensors and amount of data acquisition, and has the following technical novelties:

Signal time-shifting: In many sensing systems, relative time shifting greatly improves predictability. This phenomenon is strongly expressed in medical sensing systems. Another important observation is that cross-correlation functions are almost always unimodular. Therefore, binary search can be used for very fast calculation of the best shifts. In addition, note that the complexity of the sensor selection problem does not increase since we can always shift the selected signals by any required amount.

Signal segmentation for mutual sensor prediction: Signals in many types of embedded sensing systems have natural phases. For example: temperature and humidity are often highly impacted by sun activity, which is composed of morning, afternoon, and night phases; a heart beat has systolic and diastolic phases; and shoe pressure sensors are subject to airborne, landing, and take-off phases. Once the signals are aligned using signal time-shifting, the prediction of signals in each phase is much more accurate after segmentation, because data in one segment will otherwise often act as noise for data in another.

Subset node selection: It is easy to see that the selection of subsets of sensors from which the values of all other sensors can be computed within a given error is a NP-complete problem by observing that it can be mapped to the dominating set problem, which we solve using a novel type of constructive algorithm that facilitates an easy trade-off between the quality of the solution and the run time. Combinatorial iterative component assembly (CICA) iteratively builds a number of partial solutions that are likely to be part of the final solution. It can be easily shown that an arbitrarily close approximation can be achieved at the expense of run time. Much more importantly, CICA has very strong practical performance.

We discuss the related work in the next section, then present the low power wearable sensing system that has been the main motivation behind this study in Section 3. In Section 4, we present the signal properties of this system, which are influenced by user behavior and of which we take advantage for optimization. In Section 5, we mathematically formulate the relationships between pairs of sensors, derive the predictor-to-base sensor model, and define the predictor selection objectives. Finally, Section 7 presents experimental results and our achieved performance.

2. RELATED WORK

In this section, we briefly survey the most directly related work in (low power) sensor networks, medical and wearable sensing systems, energy optimization in body sensor networks, and sensor reading prediction.

Convergence of sensing, communication, computation, and storage technologies created the notion, testbeds, theory, and conceptual foundation for sensor networks. The research and development interest resulted in an exponentially growing number of sensor network publications. There are several conceptual and comprehensive sensor network surveys [5] [6]. From the very beginning, it was realized that energy is one the strictest constraints in many classes of sensor networks [7] [8].

With growing interest in designing sensor-based medical devices, wearable embedded sensor systems attracted an intensive and fast growing research and industrial interest [1] [9] [10] [11] [12] [13]. The emphasis has been on feasibility, processing, and interpretation of medical signals. However, energy optimization is especially important in the medical domain, where low cost and ease of every day use is crucial. Thus, it has been targeted by a range of researchers from communication and signal processing to hardware design and software engineering in body area networks [14] [15] [16] [17] [18]. There are surprisingly few reports related to cost and energy minimization for medical sensing systems. To the best of our knowledge, there are no reported techniques for simultaneous minimization of used sensors and the energy budget in wearable systems.

Exploration of the correlation of sensor readings is probably the most addressed task in embedded sensing. There are a large number of techniques ranging from a priori assumed dependency (e.g. Gaussian and random Markov fields) and similarity to movie streams [19] to non-parametric studies that exploit properties of signals such as monotonicity [20].

3. PRELIMINARIES

We will demonstrate our proposed methods for an instance of expensive systems used in medical studies for daily and ubiquitous usage. The target system is a lightweight smart shoe capable of sensing plantar pressure, movement, direction, and rotation. This system can be very attractive for a range of applications, such as instability and gait analysis outside of a laboratory environment, outdoor gaming, sports, workplace safety, and environmental data collection. In almost all of these specified applications, long term and continuous operation is required, while in an outdoor environment charging the batteries of the system is not a convenient or even possible task. High sampling rate, continuous data collection, and large-volume data transmission has introduced tremendous challenges to operating such a mobile platform. Considering the aforementioned issues, it is essential to develop a new method for instrumenting the shoe with sensors in a way that would reduce the total system's energy consumption. In Section 3.1, we explore the architecture of the designed lightweight system.

In general mobile or lightweight embedded sensing systems, wireless communication is provably one the most power hungry units in the system. In the system under study in this paper, we have used MicroLEAP as our main sensor node, which is responsible for sensing and transmitting the collected data from the sensors. Table 1 summarizes the power and energy consumption of the radio and the processor on MicroLEAP [27].

Table 1: MicroLEAP energy consumption.

	Power (mW)	Data Rate (kbps)	Energy/Bit (nJ/bit)
Processor	2.7	NA	NA
Radio	57.5	250	230

Therefore, one can easily conclude that in a network of N sensors, eliminating the sampling of a subset of the sensor data can drastically reduce the required energy consumption. Keep in mind that our goal is not to disregard the data from those sensors but provide a means to retrieve the information later on. In other words (as described in detail in Section 5), in this research one of our goals is to sample only a small subset of

Figure 1: Right: medical shoe instrumented with pressure sensors. Left: pressure sensor location map under the foot for Pedar's insole. Sensor placement and location are derived from studying Pedar's insole, which has 99 sensors

sensors, and later, in the base station, predict accurately the data values of the whole sensor network.

3.1 System Set Up and Instrumentation

The designed smart shoe is instrumented with pressure sensing material and an embedded data acquisition unit with processing and radio transmission capability. For the pressure sensing material, we either use passive resistive sensors produced by Tekscan [28] or the piezoresistive fabric produced by Eeonyx [29]. When using passive resistive sensors, sensors are placed under the insole and are connected to the data acquisition unit. In the case of the piezoresistive fabric, the fabric will be cut such that it covers the entire surface under the foot, and two conductive layers will be placed on both sides of the fabric. The sensing areas are the parts of the fabric covered by conductive material on both sides. In order to record the pressure values, the sensing area will be connected to the data acquisition board. The processing unit samples data from pressure sensors at 60 Hz. In addition to pressure sensors, the medical shoe also has gyroscopes and accelerometers, which are used for activity recognition, motion tracking, and gaming applications.

Sensor placement, especially for resource-constrained systems, requires sufficient understanding of the environment where the sensors are being deployed so that (1) *decisive and important* areas are covered and (2) resource usage is done intelligently, meaning one does not deploy more resources than necessary. Therefore, we require a deeper understanding of the pressure distribution and behavior beneath the foot so that we can meet all the required objectives and system constraints for sensor placement. These objectives can include energy requirements, sampling accuracy, coverage, etc.

To better understand the signals resulting from the exertion of pressure by both feet, we use a plantar pressure mapping system that covers the entire surface under the foot. The advantage of using such a system is that it gives us a clear picture of the complete pressure distribution under the foot. Pedar [30] is an accurate and reliable pressure distribution measuring system for monitoring local loads between the foot and the shoe. It is comprised of insoles equipped with a grid of 99 pressure sensors, which cover the entire area under the foot, and a data acquisition unit capable of data sampling and transmission to a PC over a wireless (bluetooth) connection. Even though systems such as Pedar can provide complete information about the plantar pressure, high data sampling and transmission rates make systems such as Pedar unpopular for low power applications, due to the short lifetime of the system.

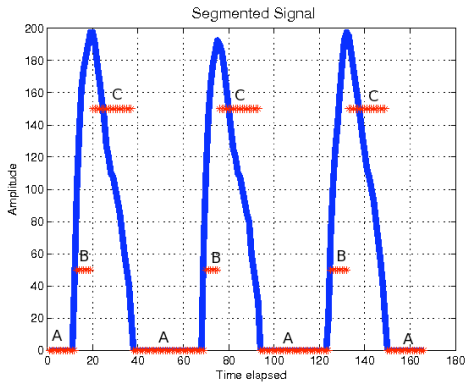

Figure 2: Three steps with three extracted states each: (A) airborne, (B) take-off, and (C) landing.

4. SIGNAL PROPERTIES

We study plantar pressure signal properties corresponding to human ambulation in order to identify physiological and behavioral trends. The extracted patterns and signal semantics, along with behavioral properties, are used in this study to model the relationship among plantar pressure signals.

A plantar pressure signal can be segmented based on its behavior, which is imposed by human gait characteristics. We divide each step into three segments: (1) airborne; (2) landing; and (3) take-off. Figure 2 demonstrates the extracted segments in the plantar pressure signal. The airborne state is defined as the time during which a particular foot is not touching the ground. The landing state is defined as the time from when the signal starts increasing its amplitude from the base offset value (calibrated zero pressure) until exactly before it starts decreasing its value; the landing state for each part of the foot, then, is the time during which the body's weight is applied to that particular sensor. Finally, the take-offs tate is the time interval during which the signal's amplitude decreases from its peak to the base offset value.

Pressure signal characteristics such as morphology, amplitude, and pattern are influenced by an individual's physiology and walking behavior. For example, Figure 4 shows pressure readings from all 99 sensors recorded from Pedar for two test subjects, two steps each, where one had flat feet and the other had hollow feet. As the figure suggests, the active pressure area is greater for the flat-footed person, while the amplitude difference between the active pressure and passive pressure areas for the hollow-footed person is much higher. Furthermore, the pressure patterns and signal morphology are almost the same in each step for the same test subject though different between the two. It is important to note that the morphological similarity will not be guaranteed if the test subject changes the type of ambulation (e.g. walking, jumping, or standing), even though it is consistent within the same type of activity.

Furthermore, the maximum amplitude of a signal is dependent on the relative position of the sensor to the person's center line of pressure progression under the feet; sensors closer to the center line of pressure will record higher pressure values compared to those that are located at the border of the active and passive pressure areas. Sensors that are located on the center line of pressure or on the lines parallel to it demonstrate almost identical behavior but at different times. Therefore, we can divide the sensors in the active pressure area

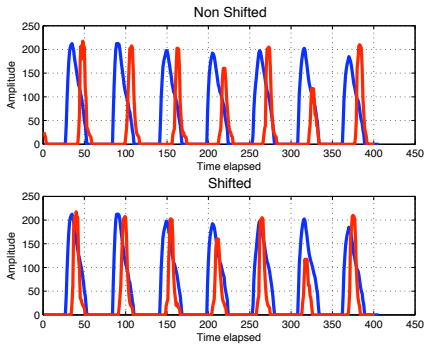

Figure 3: Top: base and predictor signals at original times. Bottom: base signal time-shifted toward predictor signal, where resulting signals are almost identical.

into sets, where data extracted from all sensors in the same set have similar morphology and almost identical shape when shifted. This implies that the signal's behavior is propagating in the walking direction onto different sensors in the same set. We take advantage of consistent progression in data modeling and predictor selection. Figure 3 shows two signals at their original times and when one is shifted toward the other.

5. PREDICTION MODELING

In order to predict the behavior of the sensors from each other, it is essential to use a good prediction model to minimize prediction errors. Due to sensors' diverse locations and their behavior under the foot during human motion, it is impossible to have a single fitting model to be used as the prediction function across sensor pairs. Therefore in order to avoid cost and complexity of managing many prediction models, we take advantage of shifting signals. Due to consistent propagation of applied pressure under the active pressure sensing area, there exists a shift for a potential base sensor toward the predictor sensor's direction, which will align two sensor values such that they will have an overlap between their landing and take-off states. Our measurements show that once a base sensor is shifted toward a predictor sensor such that there is an overlap among their landing and take off states, we will need 3 different mathematical models to present the best prediction function between any pair of sensors. The first fitting model is a linear function, while the other two are isotonic. The linear model is the best predictor when two sensors have complete overlap between landing and take-off states. The other two isotonic models, which are composed of piecewise linear and quadratic models, are the best predictors when take-off and landing states of the base and predictor sensors are not completely aligned together, and either or both are aligned with the other's airborne state.

Figure 5 demonstrates the fitted linear curve, and the isotonic curves, which illustrate the mathematical relationship between values from two different sensors, namely the *predictor* and *base sensor*.

5.1 Prediction Error

We have considered two objectives for prediction accuracy while fitting the data using the above specified prediction functions. The first objective was to create the model such that it minimizes the sum of the squares of the residuals as described in Equation 1, which is basically the least-squared method (ls). The second objective was to minimize the sum of the absolute values of the residuals as described in Equation 2, otherwise known as the L1-model.

$$minimize(sqrt\sum_{t=1}^{m} r(t)^2) \tag{1}$$

$$minimize(\sum_{t=1}^{m} |r(t)|) \tag{2}$$

We evaluate the whole process of sensor predictor selection using both of these error definitions.

5.2 Predictor Selection Objectives

Our proposed methodology in this section is aimed at selecting a potentially small subset of deployed sensors along with prediction functions such that by only utilizing that small set of sensors, all sensing data can either be measured directly or predicted with an acceptable error bound. Consider two sensors s_i and s_j and assume the corresponding sensor values as functions of time are denoted as $g_i(t)$ and $g_j(t)$. For every pair of sensors we create a collection of predictors $\Phi_{ij} = \{\phi_{ij1}, ...,\phi_{ijm}\}$. ϕ_{ijk} represents a predictor function for sensor s_j which is based on shifted values from sensor s_i by k samples. In other words, if the predicted value for sensor s_j is denoted by $g_j^*(t)$ we have:

$$g_j^*(t) = \phi_{ijk}(g_i(t-k)) \tag{3}$$

For a given predictor there is a prediction error associated with it. We use a different cost function for prediction error as described in Section 5.1. For instance, least square based prediction error can be presented as:

$$\varepsilon(\phi_{ijk}) = \frac{\sum_{t=1}^{T}(g_j(t) - \phi_{ijk}(g_i(t-k)))^2}{g_j(t)^2} \tag{4}$$

For a given sensing system, the prediction transform matrix is defined as below:

$$\Psi_{l\times n} = \begin{pmatrix} \ddots & & \\ & \phi_{ijk} & \\ & & \ddots \end{pmatrix} \tag{5}$$

where $l \leq n$ is the number of predictors denoted by $P = \{p_1, ..., p_l\} \subseteq S$. Now we can formally define the problem. The sensor predictor selection objective can be formulated as:

$$minimize(l = |P|) \tag{6}$$

such that:

$$\forall 1 \leq j \leq n, \exists i, s.t. \Psi_{ij} \neq \varnothing \tag{7}$$

$$\forall \Psi_{ij} \neq \varnothing, \varepsilon(\Psi_{ij}) \leq \delta \tag{8}$$

Constraint 7 guarantees that for any given sensor there is at least one predictor, whereas constraint 8 enforces that maximum prediction error for any given sensor is less than the target threshold of δ, where δ is an input to the problem defined by the user or is application driven.

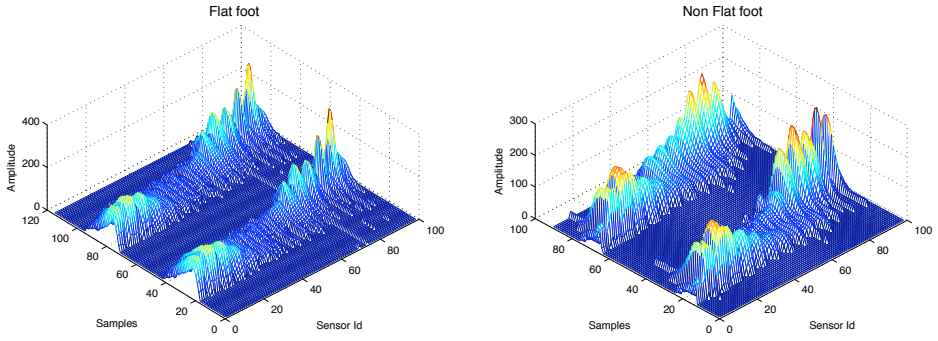

(a) (b)

Figure 4: Pressure mapping under the feet for (a) flat feet and (b) hollow feet. The progression of pressure sensors over the active pressure area is observable in both cases. The locations of sensors under the foot are based on the pressure sensor map in Figure 1.

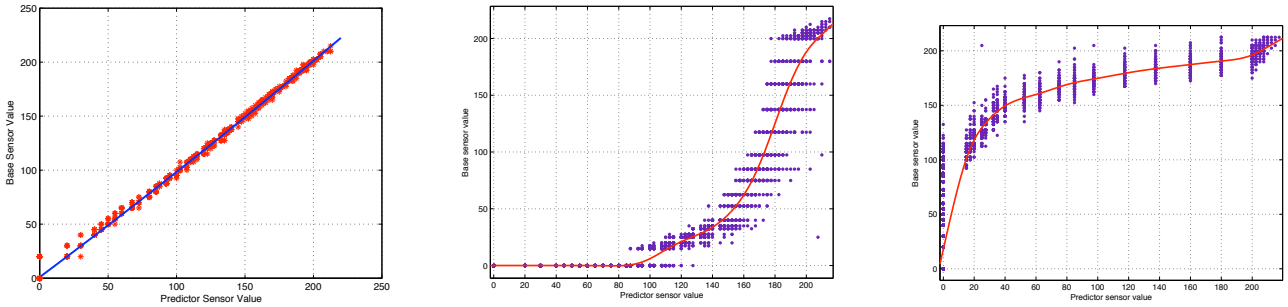

(a) (b) (c)

Figure 5: Relationship between predictor vs. base sensor when: (a) the take-off and landing states are overlapping; (b) the landing or take-off state of the base is overlapping with the airborne state of the predictor; and (c) the landing or take off state of the predictor is overlapping with the airborne state of the base.

6. OPTIMUM PREDICTOR SELECTION

In this section we cover the steps involved in the sensor selection process.

The first step of the process is to generate the prediction functions ϕ_{ijk}. Each sensor is potentially a predictor. In the context of prediction, we refer to predictor sensors as p_i and the sensors being predicted as base sensors, s_i. For a given predictor sensor p_i we generate $n \times m$ predictor functions: $\{\phi_{ijk}\}$ where $1 \leq j \leq n$ and $1 \leq k \leq m$. A prediction error corresponds to each predictor function represented as ε_{ijk}, which is computed using Equation 4. Predictor functions are generated as described in Section 5.1.

The top predictor set of sensor s_j is defined as:

$$T_j = \{p_{i_1}, ..., p_{i_k}\} s.t. \varepsilon_{p_i jk} \leq \delta \quad (9)$$

For each sensor that is a top predictor (i.e. $\forall p_i \in \cup T_j$), we create a set of base sensors for which that predictor is among the top predictors. In other words:

$$\pi_{p_i} = \{s_{j_1}, ..., s_{j_l}\}, s.t. \forall s_j \in \pi_{p_i}, p_i \in T_{s_i} \quad (10)$$

Basically, π_{p_i} represents the sensors which can be predicted by sensor i with prediction error less than δ.

6.1 Combinatorial Iterative Component Assembly

The goal in sensor selection is to find a minimal set of predictors, $\Pi = \{p_i\}$, which can be used to predict all other sensors. Formally this objective can be stated as minimizing $|\Pi|$ such that:

$$\forall s_j, \exists p_i \in \Pi, s.t. p_i \in T_j \quad (11)$$

We call this minimal setΠ^*. The way we tackle this problem is to select a minimum number of π_{p_i}s which cover the whole set of sensors. This problem is equivalent to the minimum set cover problem which is known to be NP-Hard. Therefore, we use a combinatorial iterative component assembly algorithm, or CICA, to find the min set cover. We compare the performance of CICA with a well known approximation algorithm described in [32]. In the experimental results, we show that CICA is indeed performing better than the aforementioned approximation. CICA works in the following way. First it will sort the set of predictors based on the maximum number of sensors they can cover. Then it picks the top predictors from the sorted list and combines each with the initial list to create a new predictor-to-base sensor map. This process con-

Algorithm 1 Minimum Set Cover Using Combinatorial Iterative Component Assembly

1: Input: π_{p_i} for all sensors in the system and k for top set selection threshold
2: Output:Π^* minimum set of sensors, which can be used to predict other sensors
3:$\Gamma \leftarrow$ Sort π_{p_i}s based on number of sensors they can predict in descending order and pick top K sets
4: $\Upsilon = \{\}$
5: Index = { }
6: **while** no set in Γ covers all sensors in the system **do**
7: **for** each set γ_i inΓ **do**
8: **for** each π_{p_i} from Input **do**
9: Combine covered sensors in γ_i and π_{p_i} and add the new set toΥ
10: Add predictor sensor to γ_i's corresponding index.
11: **end for**
12: **end for**
13:$\Gamma \leftarrow$ Sort sets in Υ based on number of sensors they cover in descending order and pick top k sets
14: **end while**
15:$\Pi^* \leftarrow$ Index corresponding to largest set inΓ
16: returnΠ^*

tinues until there is at least one single set which covers all the sensors. Algorithm 1 summarizes the process.

OnceΠ^* is created, we generate the Φ matrix, and the sensor selection process is completed. The way we create the elements in the Φ matrix is as follows. Rows of the matrix correspond to the predictors inΠ^* and the entries of the matrix are:

$$\Phi[p_i, j] = argmin(\varepsilon(\Psi_{p_i jk})), if p_i \in T_j \quad (12)$$

$$\Phi[p_i, j] = \varnothing, otherwise \quad (13)$$

In other words, in the column corresponding to base sensor s_i, we insert the best prediction function from its top predictors. Algorithm 2 summarizes the process.

Algorithm 2 Minimum Predictor Selection

1: Create prediction functions, ϕ_{ijk}
2: Find top predictors T_{s_i} for every base sensor s_i
3: Using T_js, create the set of base sensors (π_{p_i}) best predicted by every top predictor p_i.
4: Find the minimum set cover from π_{p_i}s and add the corresponding predictors toΠ^*
5: UseΠ^* to create the prediction matrixΦ

6.2 Generalized Sensor Selection

In general, sensor networks are deployed in a particular environment to collect specific information from that environment. Any optimization of configuration methodology will be applied to that sensor network either prior to deployment or afterward. Many of the environment-dependent offline methodologies need to be repeated if a new sensor network is to be deployed in a new place. For the case study in this paper, the sensing environment is the human body (in particular, the feet). Therefore, for any new test subject, some training data should be collected to efficiently select the best predictors and customize the system accordingly. At the same time, it is only

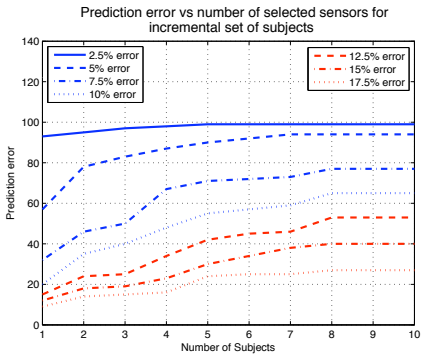

Figure 6: The number of predictor sensors converges for the generalized case.

natural to assume that, across different people, the sensing environments have some similarities that might render repeating predictor selection for any new test subject redundant. To overcome this problem, we also tried to find the globally minimum top predictors across all subjects. To achieve this, we simply modified the process as follows. We defined π_{p_i} to be:

$$\pi_{p_i} = \{s_{j_1 O_1}, ..., s_{j_l O_r}\} \quad (14)$$

where O_k represents the kth subject, and r is the total number of subjects under study. Basically, base sensors are differentiated across subjects with the secondary O_k index, but predictors remain the same. Therefore, the number of base sensors to be covered by min set cover is increased by a factor of the number of test subjects. The rest of the process remains the same.

The main question to address is: how stable are the global predictors? In other words, if the top predictors are selected based on training data from k test subjects, how will those predictors perform for the $(k+1)$th test subject? Experimentally we show that once the number of test subjects for global predictors is around 5, the corresponding predictors are in fact global and reliable for any new subject. Figure 6 shows the number of predictors for various numbers of test subjects and error rate bounds. We generated this graph by running, for a given number of test subjects (say k), the generalized predictor selection of all combinations of k test subjects for whom we had reported the average predictor size. It is clear from this graph that the predictor size converges very quickly once the number of test subjects passes 7. This means that, once the global predictor set is calculated for a few test subjects, these predictors can be reliably used for a new subject.

7. EXPERIMENTAL RESULTS

In order to illustrate the effectiveness of the proposed methodologies, we used Pedar to collect sensor data across 10 individual subjects. We tried to keep the subject set as diverse as possible in terms of walking behavior and sensor data variability. The subject set was composed of 7 men and 3 women, where one man and one woman were flat-footed and 2 men were overweight. Foot sizes ranged from 7 to 11.

For the collected data set, we performed minimum predictor selection with three different configurations: 1) least-square method for predictor function generation without any shift in base-sensor data (ls-noShift); 2) least-square method for

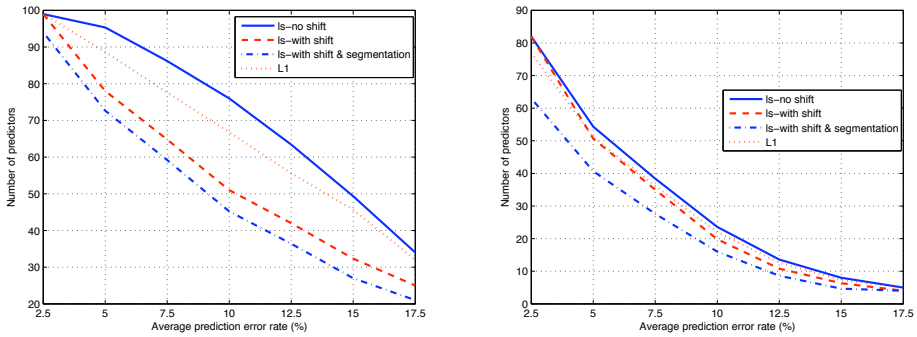

Figure 7: Number of predictor sensors vs. the average prediction error for the whole sensing network for (a) the general case and (b) averaged over individual test subjects.

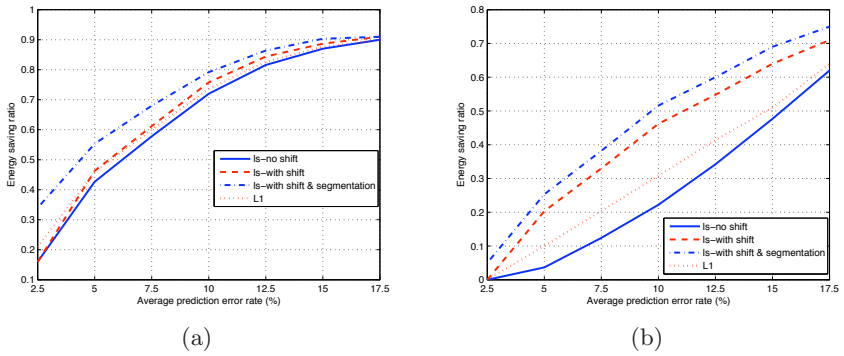

Figure 8: Ratio of energy savings with respect to no prediction vs. the average prediction error for the whole sensing network, for (a) the individual case and (b) the general case.

predictor function generation with shift in base sensor value (ls-wShift); 3) segmentation-based predictor function generation using least-square method (ls-segmentation); and 4) L1-method for predictor function generation (L1).

Furthermore, we repeated the above scenarios for the global case where the process was implemented on the aggregated data from all individuals (as described in Section 6.2). 30% of each test subject's data was used to find the best predictor, and the remaining 70% was used to evaluate the accuracy of the prediction functions. We ran the sensor selection process for a range of maximum prediction errors (δ in Equation 8). The maximum prediction error rate ranges from 2.5% to 20%. Afterwards, we simulated the estimated total energy savings on the sensor node (MicroLEAP) when the minimal predictors were used to sample the data. As seen in the system architecture, one sensor node is responsible for sampling and transmission of the data from sensors.

Table 2 summarizes the performance of the proposed combinatorial iterative component assembly algorithm to find the minimum set cover versus the greedy approach. As the table suggests, our proposed algorithm (CICA) outperforms the well known greedy algorithm in both the individual and general case. In the individual case, CICA outperforms the greedy algorithm by an average of 22.3% for error rates between 2.5% and 12.5%, while for 15% and 17.5% errors, the outcome is almost the same for both algorithms. In the general case, CICA outperforms the greedy algorithm by an average of 23.8% for error rates greater then 5%, while for 2.5% the outcome of both algorithms are the same.

Table 2: Minimum selected sensors using CICA vs Greedy algorithm

Individual			General		
Error	CICA	Greedy	Error	CICA	Greedy
2.5	63	78	2.5	94	94
5	41	52	5	65	82
7.5	21	27	7.5	59	75
10	14	18	10	42	58
12.5	11	15	12.5	42	56
15	5	6	15	24	32
17.5	4	4	17.5	21	27

Figure 7(b) illustrates the number of sensors required to predict the whole sensor network data (out of 99 sensors total) versus the maximum prediction error for the four different scenarios described above. These graphs are averaged over the 10 test subjects we had. Figure 8(a) summarizes the average power savings ratio for different maximum prediction errors. These graphs illustrate that power saving ranges from 18% to 91%, depending on the approach taken, while the maximum prediction error rate ranges from 2.5% to 20%.

Finally, we repeated the same set of experiments and simu-

lations for the general case. Figures 7(a) and 8(b) summarize the results. As expected, the general case tries to find a *global* predictor whose size is usually larger than the predictor set of an individual, and therefore energy saving ranges from 0% to 76%. Note that for a maximum prediction error rate of 2.5%, we must practically select all the sensors, resulting in no energy savings.

8. CONCLUSION

In this paper, we explored data volume management and its corresponding implications on energy consumption and system lifetime in embedded and wearable sensing systems through the introduction of multiple stages of signal analysis and optimization algorithms. The high level contribution of this paper is to study signal patterns and utilize them to develop novel *prediction* algorithms at different levels of information flow in such systems. These methods aim to make expensive wearable sensing systems more feasible for everyday use by minimizing sampling sources while enabling reconstruction of the data from all sensors. One goal was to use a subset of sensors to accurately generate the data from all sensors. This goal was achieved by introducing two novel methods for signal shifting, which enables better prediction of sensor data, followed by data segmentation to further enable piecewise predictions. To solve the above problems, we also developed an efficient approximation algorithm called combinatorial iterative component assembly (CICA) to select optimum predictors for each scenario. In order to show the effectiveness of the proposed methodologies, we applied the presented methods on an embedded wearable sensing system equipped with 100 pressure sensors. Experimental results show that the proposed techniques can yield from 56% to 96% in energy reduction while maximum sampling error rate ranges from only 5% to 17.5%.

9. REFERENCES

[1] S. C. Jacobsen, T. J. Petelenz, and S. C. Peterson, "Wireless health monitoring system," US Patent 6,160,478, 2000.

[2] R. Jafari, F. Dabiri, and M. Sarrafzadeh, "CustoMed: A power optimized customizable and mobile medical monitoring and analysis system," *ACM HCI Challenges in Health Assessment*, 2005.

[3] W. Wu, A. Baui, M. Batalin, L. Au, J. Binney, and W. Kaiser, "MEDIC: Medical embedded device for individualized care," *Artificial Intelligence in Medicine*, vol. 42, no. 2, pp. 137-152, 2008.

[4] D. Malan, T. Fulford-Jones, M. Welsh, and S. Moulton, "CodeBlue: an ad hoc sensor network infrastructure for emergency medical care," *WAMES*, 2004.

[5] D. Culler, D. Estrin, M. Srivastava, and Guest Editors, "Introduction: overview of sensor networks," *Computer*, vol. 37, no. 8, pp. 41-49, 2004.

[6] I. F. Akyildiz, T. Melodia, and K. R. Chowdhury, "A survey on wireless multimedia sensor networks," *Computer Networks*, vol. 51, no. 4, pp. 921-960, 2007.

[7] D. Ganesan, B. Krishnamachari, A. Woo, D. Culler, D. Estrin, and S. Wicker, "Complex behavior at scale: an experimental study of low-power wireless sensor networks," Technical Report UCLA/TR 02-0013, 2002.

[8] J. Polastre, J. Hill, and D. Culler, "Versatile low power media access for wireless sensor networks," *Sensys*, 2004.

[9] S. Popovic, M. R. Dietz, V. Morari, M. Pappas, I. Keller, and T. Mangold, "A reliable gyroscope-based gait-phase detection sensor embedded in a shoe insole," *IEEE Sensors Journal*, vol. 4, no. 2, pp. 268-274, 2004.

[10] W. Wu, L. Au, B. Jordan, T. Stathopoulus, M. Batalin, W. Kaiser, A. Vahdatpour, and M. Sarrafzadeh, "The SmartCane system: an assistive device for geriatrics," *Body Area Networks*, 2008.

[11] K. Oshima, Y. Ishida, S. Konomi, N. Thepvilojanapong, and Y. Tobe, "A human probe for measuring walkability," *Sensys*, pp. 353-354, 2009.

[12] V. Erickson, A. U. Kamthe, and A. E. Cerpa, "Measuring foot pronation using RFID sensor networks," *Sensys*, pp. 325-326, 2009.

[13] K. Lorincz, B. Chen, G. W. Challen, A. R. Chowdhury, S. Patel, P. Bonato, and M. Welsh, "Mercury: a wearable sensor network platform for high-fidelity motion analysis," *Sensys*, pp. 183-196, 2009.

[14] V. Leonov, P. Fiorini, S. Sedky, T. Torfs, and C. Van Hoof, "Thermoelectric mems generators as a power supply for a body area network," vol. 1, pp. 291-294, 2005.

[15] L. Yan, L. Zhong, and N. K. Jha, "Energy comparison and optimization of wireless body-area network technologies," *BodyNets*, pp. 1-8, 2007.

[16] H. Ghasemzadeh, E. Guenterberg, K. Gilani, and R. Jafari, "Action coverage formulation for power optimization in body sensor networks," *ASPDAC*, pp. 446-451, 2008.

[17] Y. Liu, B. Veeravalli, and S. Viswanathan, "Critical-path based low-energy scheduling algorithms for body area network systems," RTCSA, pp. 301-308, 2007.

[18] S. Xiao, A. Dhamdhere, V. Sivaraman, and A. Burdett, "Transmission Power Control in Body Area Sensor Networks for Healthcare Monitoring," *IEEE Communications Journal*, vol. 27, no. 1, pp. 37-48, 2009.

[19] S. Goel and T. Imielinski, "Prediction-based monitoring in sensor networks: taking lessons from MPEG," *SIGCOMM*, vol. 31 no. 5, 2001.

[20] F. Koushanfar, N. Taft, and M. Potkonjak, "Sleeping coordination for comprehensive sensing using isotonic regression and domatic partitions," *INFOCOM*, 2006.

[21] M. A. Batalin, M. Rahimi, Y. Yu, D. Liu, A. Kansal, G. S. Sukhatme, W. J. Kaiser, M. Hansen, G. J. Pottie, M. Srivastava, and D. Estrin, "Call and response: experiments in sampling the environment," *Sensys*, pp. 25-38, 2004.

[22] G. Gandhi, S. Suri, and E. Welzl, "Catching elephants with mice: sparse sampling for monitoring sensor networks," *Sensys*, pp. 261-274, 2007.

[23] M. Malinowski, M. Moskwa, M. Feldmeier, M. Laibowitz, and J. A. Paradiso, "CargoNet: a low-cost micropower sensor node exploiting quasi-passive wakeup for adaptive asynchronous monitoring of exceptional events," *Sensys*, pp. 145-159, 2007.

[24] S. Jevtic, M. Kotowsky, R. P. Dick, P. A. Dinda, and C. Dowding, "Lucid dreaming: reliable analog event detection for energy-constrained applications," *IPSN*, pp. 350-359, 2007.

[25] P. Wan and M. D. Lemmon, "Event-triggered distributed optimization in sensor networks," *IPSN*, pp. 49-60, 2009.

[26] J. Liu, P. Cheung, F. Zhao, and L. Guibas, "A dual-space approach to tracking and sensor management in wireless sensor networks," *WSNA*, 2002.

[27] L. K. Au, W. H. Wu, M. A. Batalin, D. H. Mclntire, and W. J. Kaiser, "MicroLEAP: energy-aware wireless sensor platform for biomedical sensing applications," *BIOCAS*, pp. 158-162, 2007.

[28] Tekscan pressure sensor. http://www.tekscan.com.

[29] Eeonyx resistive fabric. http://www.eeonyx.com.

[30] Pedar: plantar pressure system. http://www.novel.de.

[31] L. Klingbeil and T. Wark, "A wireless sensor network for real-time indoor localisation and motion monitoring," *IPSN*, pp. 39-50, 2008.

[32] P. Slavik, "A tight analysis of the greedy algorithm for set cover," *STOC*, pp. 435-441, 1996.